IAC-06-C1.2.08

SPACECRAFT OPTICAL BEAM POINTING AND JITTER CONTROL

Brij N. Agrawal*
Spacecraft Research and Design Center
Department of Mechanical and Astronautical Engineering
Naval Postgraduate School
Monterey, CA 93943, USA
E-mail:agrawal@nps.edu

ABSTRACT

This paper presents the recent results on research in acquisition, tracking, and pointing of spacecraft at the Spacecraft Research and Design Center. In acquisition, the results are presented on minimizing slew time by optimizing the orientation of the three control moment gyro array. In spacecraft pointing, the results are presented on minimizing jitter control. Several control techniques, such as Least Mean Square (LMS) and Linear Quadratic Regulator (LQR) were applied for jitter control. Improvement in LMS techniques to improve convergence rate was achieved by adding Adaptive Bias Filters (ABF) to the reference signal. In the experiments, the platform is vibrated at 50 and 87 Hz. In addition, a fast steering mirror is used to inject a random component of 200 Hz band-limited white noise. The experimental results demonstrated that the addition of ABF to LMS significantly increased the converging rate of the jitter. In order to achieve the reduction of both sinusoidal and random jitter, a combination of ABF/LMS and LQR is most effective.

1. INTRODUCTION

For many future space missions, such as imaging and laser communications, the optical beam pointing requirements will be in sub-micro-radians and the jitter requirements in nano-radians. In order to achieve these performance requirements, the spacecraft attitude control is divided into two parts: large angular motion and coarse pointing is provided by the spacecraft bus and fine pointing is provided in the optical payload by fast steering mirrors. The complexity is further increased because some of these missions will require large aperture telescopes in the range of 10-30 m diameter and fine surface control. Therefore, improved technologies have to be developed to achieve these performance requirements for acquisition, tracking and pointing of spacecraft.

At the Spacecraft Research and Design Center (SRDC), Naval Postgraduate School, several projects have been undertaken to develop these technologies for acquisition, pointing and jitter control. These projects have resulted in the development of several test beds to validate these new technologies. Schwartz [1] has provided a review of spacecraft attitude control simulators. The major project at SRDC has been Bifocal Relay Mirror Spacecraft (BRMS). The BRMS is composed of two optically coupled telescopes used to redirect a laser beam from ground, aircraft, or space based laser to distant points on the earth or in space. The receive telescope captures the incoming laser beam and the transmit telescope directs the beam to the desired points. The complexity in the control is increased because both

* Distinguished Professor, Director, Spacecraft Research and Design Center

telescopes have similar pointing and jitter requirements, moving independently, and have dynamic interaction between them with changing spacecraft inertia.

This paper presents the recent results on research at the center in acquisition, tracking, and pointing of spacecraft. In acquisition the results are presented on minimizing slew time by optimizing the orientation of three control moment gyro array. In spacecraft pointing, the results are presented on minimizing jitter control.

2. BIFOCAL RELAY MIRROR SPACECRAFT TESTBED

Figure 1 illustrates the concept of the experimental test bed for the BRMS. The three-axis spacecraft bus simulator on the right employs the optical payload including optically coupled receive and transmit telescopes. The laser beam from the laser source on a Moving Target-Source Test Fixture (MTSTF), at left, is received by the top telescope and transmitted by the bottom telescope (fixed to the bus) to the target on the MTSTF. The top and bottom telescopes are connected by the one axis rotational joint.

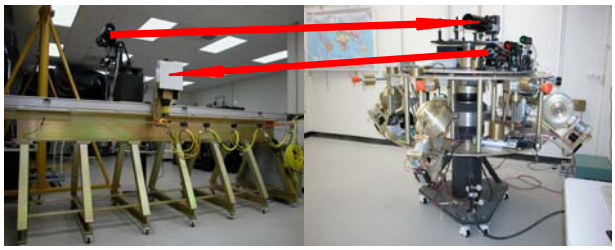

Fig 1: Test Bed for Bifocal Relay Mirror Spacecraft

Figure 2 shows the spacecraft simulator [Refs. 2-3]. The spacecraft bus simulator is supported on a spherical air bearing to simulate a weightless environment. A thin film of compressed air is injected between a spherical ball and a mating spherical cup. This provides three axis motion of the spacecraft without friction. The gravitational torque will be zero on the spacecraft, simulating space environment, if the spacecraft center of mass is on the center of rotation of the spherical ball. Automatic balancing is introduced to achieve this balancing. The simulator has three variable speed control moment gyros (CMGs), Inertial Measurement Unit (IMU), two inclinometers (roll, pitch), on-board computer, IR sensor, and magnetometers for navigation and attitude control. IMU consists of 3 Fiber Optics Rate Gyroscopes with integrated 3 translational accelerometers. Variable Speed Control Moment Gyroscopes (VSCMGs) are selected as main attitude control actuators for its high torque capacities. Each CMG has a maximum angular momentum of 22.5 N-m-s and a maximum torque of 12 N-m.

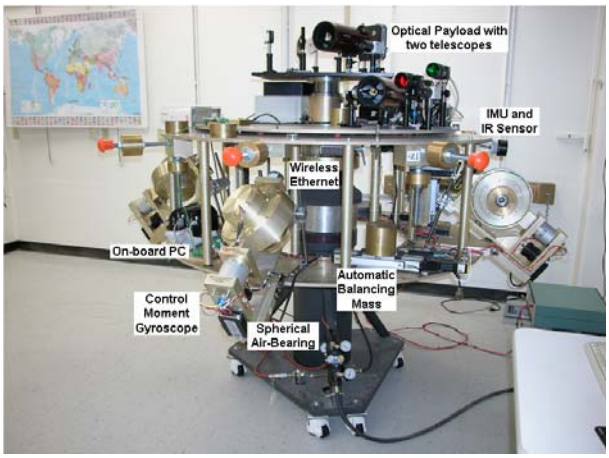

Fig 2: Three Axis Spacecraft Simulator with Optical Payload

The optical payload of the simulator consists of receive telescope on the upper deck and the transmit telescope on the lower deck.

3. CONTROL MOMENT GYROSCOPE ARRAY CONFIGURATION

Control Moment Gyros (CMGs) are momentum exchange device which generate control torque for spacecraft attitude control.

The change in the direction of the momentum built by the CMG flywheel has the amplification effect of the torque generated. Therefore, high torque can be generated efficiently with CMGs. For the BRMS, CMGs are preferable actuation devices due to the high speed slew capability. In order to create a three dimensional torque, at least three CMGs are required. The collection of these CMGs is called a CMG array. The geometrical configuration of the CMG array determines the characteristics of the momentum space for the spacecraft control. For a single gimbal CMG array, there are many different CMG configuration types such as symmetric type, pyramid type, Skew type, and Multiple type. MIR spacecraft, for example, utilizes symmetric type with 6 CMGs. For a large slew maneuver control of a spacecraft with this CMG array, the main difficulty arises from the singularity of the CMG array.

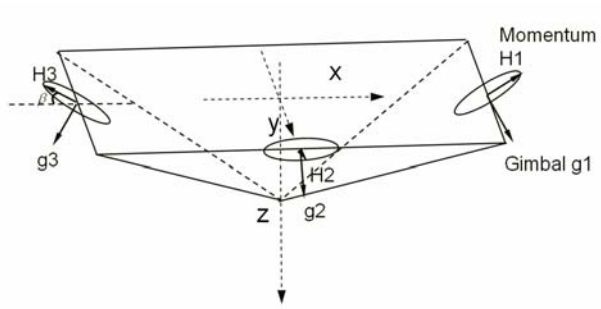

Fig 3: CMG Array Configuration of TAS2

Considering the current configuration of simulator shown in Figure 3 with constant speed CMG operation (200 rad/sec), the total momentum from this CMG array geometry is written as

$$\mathbf{h} = \begin{bmatrix} -\cos\beta\sin\delta_1 \\ \cos\delta_1 \\ \sin\beta\sin\delta_1 \end{bmatrix} + \begin{bmatrix} -\cos\delta_2 \\ \cos\beta\sin\delta_2 \\ \sin\beta\sin\delta_2 \end{bmatrix} + \begin{bmatrix} \cos\beta\sin\delta_3 \\ -\cos\delta_3 \\ \sin\beta\sin\delta_3 \end{bmatrix} \quad (1)$$

where β is the skew angle in Figure 3, δ is the gimbal angle of the ith CMG (I = 1,2,3), and angular momentum from single CMG is normalized to 1 CMG worth of momentum. Then the torque from the CMG array becomes the time derivative of the total CMG momentum, which can be written as a matrix form such that

$$\dot{\mathbf{h}} = A\dot{\delta} \quad (2)$$

where,

$$A = \begin{bmatrix} -\cos\beta\cos\delta_1 & \sin\delta_2 & \cos\beta\cos\delta_3 \\ -\sin\delta_1 & -\cos\beta\cos\delta_2 & \sin\delta_3 \\ \sin\beta\cos\delta_1 & \sin\beta\cos\delta_2 & \sin\beta\cos\delta_3 \end{bmatrix} \quad (3)$$

when the matrix *A* becomes singular, no control torque can be generated for the commanded control torques. Singularity surface plot is a useful tool to visualize the singularity states in the momentum space.

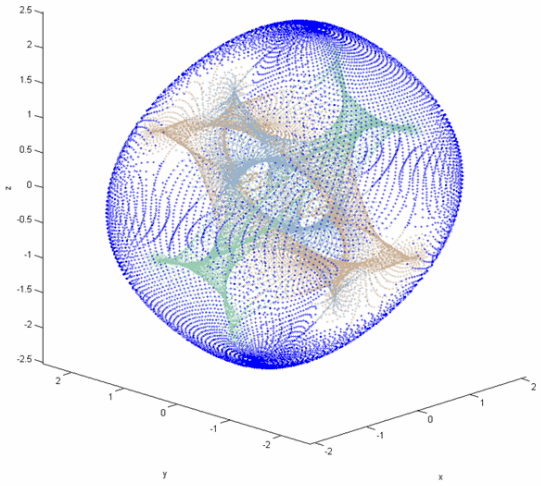

Fig 4: Singularity Surface of 3 CMG Array β= 57 degrees (momentum from each CMG normalized to 1)

Figure 4 shows the singularity surface of 3 CMG pyramid type array with the skew angle of β = 57 degrees. This singularity surface represents the case where the matrix A becomes singular in the momentum space. The outer surface of the singularity surface represents the angular momentum envelop. This is the border of the maximum work space with this specific CMG array. The control law has to be designed such that the CMG steering avoids this singularity surface. With 3 CMGs, it is difficult to avoid internal singularities because of the lack of redundant degrees of freedom. If the CMGs are restricted to operate in the singularity free

region, the bigger singularity-free volume space, the better. We are trying to find CMG array geometry with maximum available singularity-free momentum space. With this 3 CMG pyramid-type configuration with the skew angle of 57 degrees, internal singularity occurs near zero momentum. Therefore, it is not the best CMG array configuration with 3 CMGs.

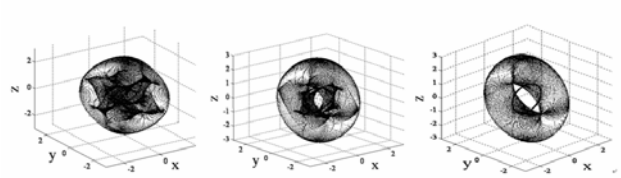

Fig 5: Singularity Surface of 3 CMG Array (Left: β = 70 degrees, Middle: β = 80 degrees, Right: β = 90 degrees)

Figure 5 shows how the singularity surface changes with the different values of skew angle. As skew angle increased to 90 degrees, the singularity volume becomes larger. In order to study the singularity free volume with respect to the skew angle, determinant of matrix *A* is computed to find out when the singularity occurs. Then the minimum singularity angular momentum magnitude is computed with respect to the skew angle as shown in Figure 16. It can be shown that when the skew angle is 90 degrees, the CMG array will have a largest singularity-free angular momentum space of 1*H* (*H* being momentum of single CMG) for any direction from the origin.

It can be seen from Figure 5 that although skew angle of 90 degrees has a minimum singularity-free angular momentum of 1H, there exists 2H (radially) singularity free momentum space in y direction. Therefore, the CMG array configuration can be modified to have a larger singularity-free momentum volume for certain desired direction. In our BRMS testbed, z-axis rotation (yaw maneuver) requires larger momentum volume for relaying operation than the other axes.

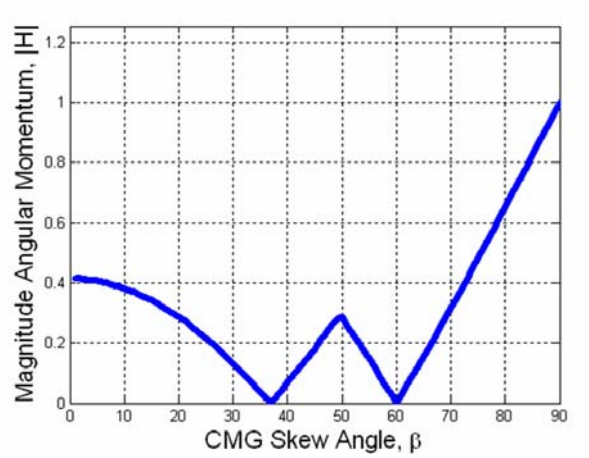

Fig 6: Minimum Momentum vs. Skew Angle

Figure 7 shows the comparison between skew angle of 90 degrees and mixed skew angles of (90, 0, 90) degrees. The singularity surface has been rotated to have ±2H singularity-free momentum space in z direction. Slew maneuver experiments are carried out to verify these results.

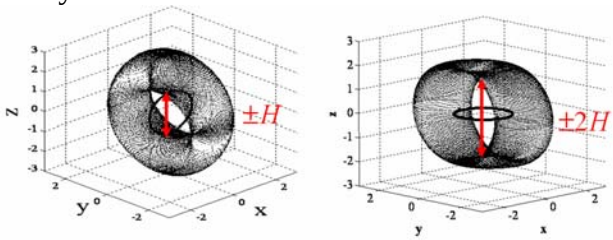

Fig 7: Singularity Surface of 3 CMG Array (Left: β = (90 90 90) degrees, Left: β = (90 0 90) degrees)

For the left plot in Figure 8, momentum trajectory of 4 second, 5 degree yawing maneuver followed by 4 second, -5 degree slew maneuver is shown along the z-axis. The momentum trajectory also shows y direction trajectory due to the center of gravity offset, while the test bed is regulated at zero attitude after the slew maneuver. In right plot in Figure 8, the test bed was able to slew 13 degrees in 4 seconds without hitting the singularity surface due to the increased singularity-free momentum volume along z-axis.

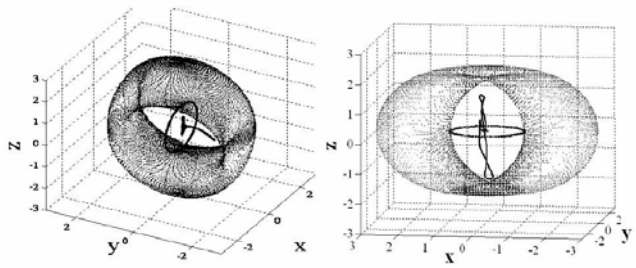

Fig 8: Momentum Trajectory from Experiment (Left: β = (90 90 90) degrees, Left: β = (90 0 90) degrees)

4. JITTER CONTROL

In order to achieve jitter control , several techniques have been proposed, including adaptive control systems such as the Least Means Squares (LMS), Model Reference or adaptive lattice filters [4]-[7]. Each of these adaptive systems requires a reference signal in order to reject the disturbance. An experimental Laser Jitter Control (LJC) Test bed has been developed to test various control techniques on vibrationally induced jitter.

Control Methods

Least Means Squares (LMS) Algorithm

The LMS algorithm is one of the simplest yet robust adaptive algorithms. In the LMS algorithm, we adjust the *tap gains* based on the response of the system to (1) the error, (2) a reference signal correlated with the disturbance, and (3) the control input. The algorithm uses the method of Least Squares to find the optimum values for the tap gains. In particular, the algorithm relies on *predicting* its next input, which is simply the disturbance in the case of laser jitter control, to optimize the *tap gains*. The error - the difference between the predicted signal and the system output - is then used to recalculate the gains that minimize the error in return. For the LJC Testbed, the feed-back or target detector is used to provide the error signal, and the feed-forward detector provides the correlated disturbance input signal. This type of control algorithm not only calculates the necessary gains, but also identifies the system, simplifying the requirement to mathematically model the system. The type of adaptive control employed in the experimental setup utilizes predictors. The predictor used in this algorithm is the discretized transversal or ladder filter, as shown in Figure 9.

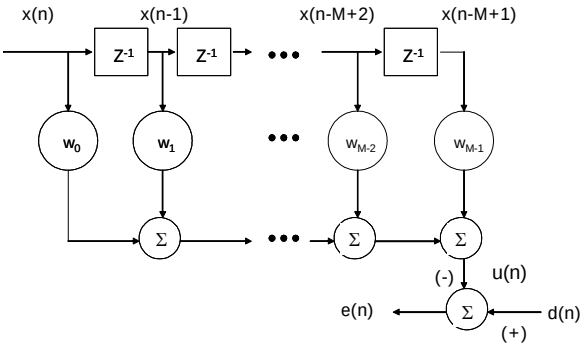

Fig. 9: Transversal Filter

The filter has M stages and the input, or reference signal is x(n). x(n) is delayed one time step for each of the M stages, with the exception of the current input. The tap gains, w_m multiply this vector of delayed inputs and the products are summed together to develop the control input to the mirror. The desired input, or d(n) is that mirror motion that cancels any motion in the laser beam caused by the supporting structure and equipment. The error is the difference between the target center and the laser beam's position. The tap gains are adjusted by means of the update equation:

$$\bar{w}(n+1) = \bar{w}(n) + \mu \bar{x}(n) e(n) \qquad (4)$$

where μ is the step size that controls the stability of the algorithm and the overbar denotes a vector. In words, equation (4) states that the vector of tap gains, $[w_0, w_1, \ldots w_{M-1}]^T$ at time n+1 is updated by the vector of tap gains at time n, adjusted by the error

(e) at time n, multiplied by the vector of delayed inputs at time n, $[x(n), x(n-1), \ldots, x(n-M+1)]^T$ and the adaptation step size μ.

Filtered-X LMS Algorithm

In any practical laser targeting or relay station, there is a secondary path through which the output of the LMS filter must go. In this case, Fast Steering Mirrors (FSM) and related optics are used to correct the beam. This secondary path must be modeled in the control algorithm in order to take into account the delays and other effects that occur to the control signal. In order to properly make use of the LMS algorithm, a copy of the secondary plant transfer function is placed in the path to the updating algorithm for the weight vector. This is known as the Filtered-X LMS (FXLMS) algorithm and was derived by Widrow [8]. The block diagram for the use of this algorithm with the LJC Testbed is provided below:

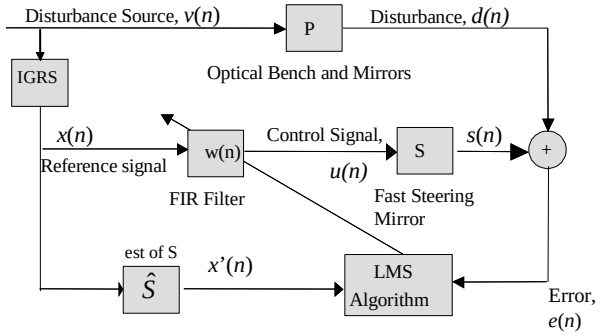

Fig 10: Block Diagram of the FXLMS Control system.

The control input to the FSM is the output $u(n)$ of the FIR filter adapted by the LMS algorithm in Fig. 9, using a reference signal x' that has been filtered by a copy of the secondary plant transfer function :

$$u(n) = \bar{w}^T(n)\,\bar{x}'(n) \qquad (5)$$

where $\bar{x}'(n) = \hat{\bar{s}}(n) * \bar{x}(n)$, with $\hat{\bar{s}}(n)$ the vector of FIR coefficients that model the secondary path. The error between the desired signal, (i.e. the jitter in the beam) and the beam's motion as compensated by the FSM is then:

$$e(n) = d(n) - s(n) \qquad (6)$$

where $s(n)$ is the pseudo-output of the FSM, since the output of the FSM is the actual beam position in the practical situation. This error is then used in the update equation for the tap gains (equation (4)).

The Adaptive Bias Filter (ABF)

Using a one or two weight LMS filter, the bias in the reference signal is adjusted to remove the DC component of the error signal. An estimate of *C'* is used as the reference signal to the ABF. The error signal in this case is the mean error, which stops the adaptation once the signal is centered on the target.

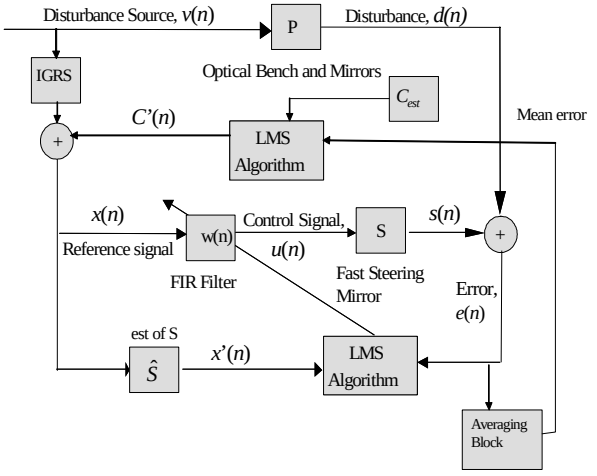

Fig. 11: Block diagram of ABF modification

Laser Jitter Control Testbed

The Laser Jitter Control (LJC) Test bed is located in the Spacecraft Research and

Design Center - Optical Relay Mirror Lab at the Naval Postgraduate School in Monterey CA. The components are mounted on a Newport Optical Bench which can be floated in order to isolate the components from external vibrations. The idea is to simulate a satellite or vehicle "bus" which houses an optical relay system. The laser beam originates from a source and passes through a Disturbance injection Fast Steering Mirror (DFSM). The DFSM corrupts the beam using random or periodic disturbances simulating the disturbances that might occur as a result of the transmitting station or the tip and tilt the beam may suffer as it passes through the atmosphere. A vibration isolation platform is used to mount the relay system, and to isolate the relay system from the optical bench. The relay system platform may be vibrationally disturbed by a 5 lbf inertial actuator, simulating on-board running equipment such as control moment gyros, reaction wheels, cryo-coolers, etc.

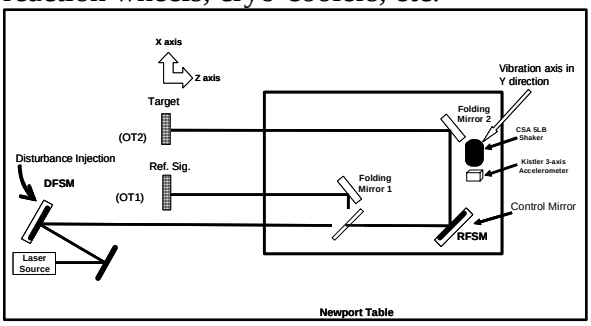

Fig. 12 Laser Jitter Control Testbed

The incoming beam is split and reflected off the platform to a Position Sensing Detector (PSD) in order to obtain a reference signal that indicates the on-board and injected disturbances. It is recognized that this is not a normal means to measure the disturbances as one would not be able to mount a PSD off the 'bus'. However, this reference PSD may be seen as simulating an on-board Inertial Measurement Unit (IMU), which is normally available in satellites with an optical payload. Using an accurate and sensitive IMU and a PSD, one could determine a similar reference signal. This setup allows a comparable measurement without the added cost of an IMU. A control FSM, designated the Receive FSM or RFSM, is used to correct the disturbed beam. The corrected beam is then reflected off the platform by a second folding mirror to the target PSD. A block diagram of the system is shown below, as well as a picture of the actual setup.

Fig. 13: Laser Jitter Control Testbed

Experimental Results

In this experiment, the platform is vibrated by the inertial actuator at the two frequencies 50 and 87 Hz. In addition, a fast steering mirror is used to inject a random component of 200 Hz band-limited white noise, to simulate the effect of atmospheric turbulence on the uplink laser beam for a simulated relay station. Since the LMS controller uses an Internally Generated Reference Signal (IGRS) consisting of the two disturbance frequencies, the controller will not remove the random component. However, by combining the LMS controller with the LQR, control of the random component as well as the frequencies added by the inertial actuator may be realized. Additionally, by adding the ABF modification and removing the integrator from the LQR, a faster response to the bias error may also be achieved. A comparison of

three experiments using the different control methods is shown below.

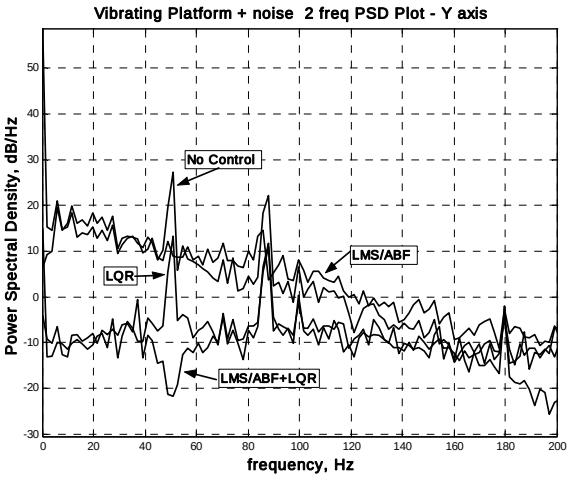

Fig. 14: Y axis PSD plot of the 2 frequency vibrating platform experiment.

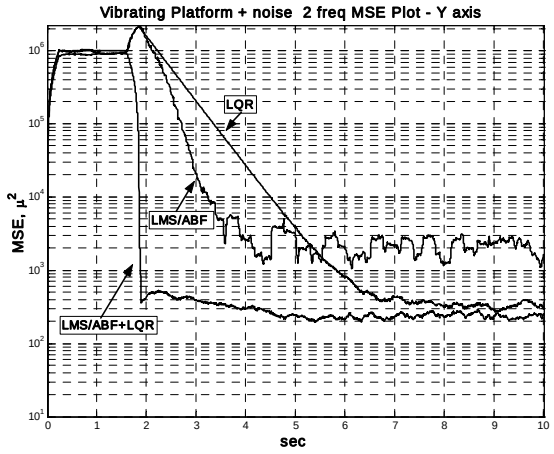

Fig. 15: Y axis MSE plot of the 2 frequency vibrating platform experiment

5. CONCLUSIONS

Based on these results, the following conclusion can be reached. For three CMGs array, 90 degree skew angle provides the maximum singularity free volume. The minimum singularity free angular momentum is 1 H ,where H is angular momentum of one CMG, and maximum singularity free angular momentum is 2 H in one direction. It has been shown that if the spacecraft slew only in one direction, similar to our test bed, the skew angles of the CMGs can be determined to get 2H singularity free momentum in that direction.. For the jitter control, based on the experiment results, it can be concluded that the addition of ABS filter to LMS significantly increased the converging rate of jitter. LMS is most effective for sinusoidal jitter and LQR for random jitter. In order to achieve the reduction of both sinusoidal and random jitter, a combination of ABS/LMS and LQR is most effective.

6. REFERENCES

[1] Schwartz, J. L., Peck, M. A., and Hall, C.D., "Historical Review of Spacecraft Simulators", Proceedings of the AAS/AIAA Spaceflight Mechanics Meeting, No. AAS 03-125, Ponce, Puerto

[2] Romano, M., Agrawal, B. N., "Attitude Dynamics/Control of Dual-Body Spacecraft with Variable-Speed Control Moment Gyros", AIAA Journal of Guidance, Control, and Dynamics, vol. 27, No. 4, pp. 513-525, July-August 2004.
Rico, Feburary 10-13, 2003.

[3] Agrawal, B. N., Kim, J.-W., Romano, M., "Attitude Control and Determination of the NPS Bifocal Mirror Testbed," 55th International Astronautical Conference, Vancouver, Canada, 2004.

[4] Skormin, V.A., Tascillo, M.A., and Busch, T.E., "Adaptive jitter rejection technique applicable to airborne laser communication systems," Optical Engineering, Vol. 34, pp. 1267, May 1995.

[5] Skormin, V.A. and Busch, T.E., "Experimental implementation of model reference control for fine tracking mirrors," Proceedings of the SPIE Vol. 2990, pp. 183-189, February 1997.

[6] Glaese, R.M., Anderson, E.H., and Janzen, P.C., "Active Suppression of Acoustically Induced Jitter for the Airborne Laser," Proceedings of the SPIE Conference on Laser Weapons Technology, SPIE paper 4034-19, pp. 157-162, April 2000.
[7] Boelitz, F.W., Gibson, J.S., Walter, R.E. and Washburn, D.C., "Active Vibration Cancellation for ABLE ACE," Unpublished.
[8] Widrow, B., Shur, D. and Shaffer, S. "On adaptive inverse control," Proceedings of the 15th Asilomar Conference, pp. 185-189, 1981.